Computational Transonic Optimization and Wind-Tunnel Test of a Semispan Wing

H.P. Haney* and E.G. Waggoner†
Vought Corporation, Dallas, Texas
and
W.F. Ballhaus‡
NASA Ames Research Center, and Aeromechanics Laboratory, U.S Army Aviation R&D Command, Moffett Field, Calif.

A computational transonic wing design procedure has been developed and verified by a wind-tunnel test of a variable camber semispan wing model. The Bailey-Ballhaus transonic potential flow analysis code linked to Vanderplaat's constrained minimization routine was used to optimize test configurations at 0.9 Mach number. Based on wind-tunnel test results, computationally optimized designs were as efficient as the best configurations determined by previous parametric testing and performed better at off-design points. Wind-tunnel wing pressures agreed well with predictions from the improved Bailey-Ballhaus code at moderate C_L's. Computational optimization was shown to be an effective transonic wing design tool.

Nomenclature

AR	= aspect ratio
$b/2$	= exposed semispan length, 106.68 cm (42 in.)
C_L	= lift coefficient, lift/qS
$C_{L_{exp}}$	= experimental lift coefficient
C_p	= pressure coefficient, $(p-p_\infty)/q$
ETA	= wing semispan station, $y/(b/2)$
M	= Mach number
p	= local static pressure, psf
p_∞	= freestream static pressure, psf
q	= freestream dynamic pressure, psf
S	= wing reference area, 0.6 m^2 (6.447 ft^2)
U	= local flow velocity
U_∞	= freestream velocity
x/c	= nondimensional wing chord station
y	= spanwise distance from semispan root, cm (in.)
α	= wing angle of attack
δ_i	= flap deflection angle
$\Lambda_{L.E}$	= wing leading-edge sweep
λ	= wing taper ratio

Introduction

VOUGHT Corporation and NASA Ames Research Center began a cooperative effort in 1973 to apply transonic potential flow analyses to practical design problems and compare predictions with experiment. It was hoped that this work would establish guidelines for computational wing design and also identify areas where improvement was needed in the analysis codes. In 1975, Vought and NASA Ames began a joint effort to develop wing optimization procedures and to verify them experimentally. Camber distributions for Vought's variable camber semispan wing model were defined using a transonic analysis code combined with an optimization procedure. The designs were tested in the NASA Ames 14-ft transonic tunnel and compared against results from previous design studies on the wing.

Presented as Paper 78-102 at the AIAA 16th Aerospace Sciences Meeting, Huntsville, Ala., Jan. 16-18, 1978; submitted March 6, 1978; revision received May 30, 1978.

Index categories: Transonic Flow; Computational Methods; Aerodynamics.

*Engineering Specialist, Flight Technologies. Member AIAA.
†Lead Engineer, Flight Technologies. Member AIAA.
‡Research Scientist. Associate Fellow AIAA.

Wing Optimization Procedure

One of the major advantages of numerical solutions in relation to experimental testing is the relative ease of modifying a configuration. This capability enables a designer to investigate many configurations or perturbations to a given configuration in a relatively short time. With this added flexibility, a design problem can then be thought of in different terms. Preliminary analysis may initially encompass a much larger design space, thereby increasing the possibility of the target design being in the design space. The space may then be reduced computationally to a size that is commensurate with the accuracy and validity of the computational tool. Experimental refinement and verification are then performed in a much smaller design space, reducing both the cost and time required.

The wing design problem may be solved computationally by tying the analysis tool to a numerical optimization procedure. Basically, this involves systematic perturbation of certain geometric design variables to arrive at an optimum configuration relative to some specific object parameter (e.g., minimum drag at a certain lift, pressure gradient at a specific chordwise location, etc.). This approach was taken by Hicks[1] at NASA Ames for optimizing airfoil contours. Linking a two-dimensional compressible flow analysis routine to an optimization technique, he was successful at optimizing airfoil geometries for both subsonic and transonic design conditions.

The next logical step is to extend the optimization to three dimensions and to identify effective wing design procedures. The objective of this study has been to develop a three-dimensional optimization approach, apply it to several wing design problems, and verify the resultant designs through experimental testing. Vought's variable camber semispan wing model was chosen for the design study because of the flexibility afforded by its unique design. The wing is characterized by multisegmented leading- and trailing-edge flaps whose hinge lines are skewed relative to the leading and trailing edge of the wing (see Fig. 1). An extensive range of spanwise camber and twist variations is obtainable by varying the segmented flap deflections. A highly instrumented model employing the skewed hinge line concept had been constructed and tested in NASA Langley's 8-ft transonic tunnel[2] for preliminary assessment of the aerodynamic characteristics. Many transonic analysis runs were made in a parametric computational study to define the configurations for testing.

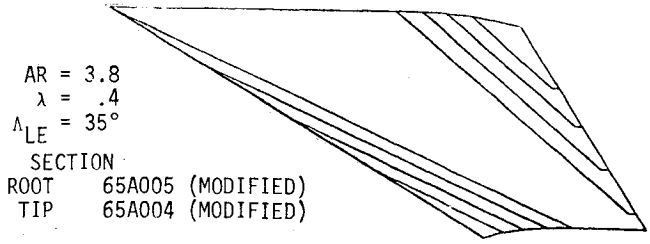

Fig. 1 Oblique view Vought variable camber wing.

The difficulty and expense of this exercise highlighted the need for a more systematic and streamlined design procedure.

An analytical design procedure was formulated by utilizing potential flow wing analysis techniques and numerical optimization within the geometric constraints of the variable camber wing. The Bailey-Ballhaus transonic potential flow[3,4] and Woodward-Carmichael linear potential flow analysis[5] codes were linked to Vanderplaat's constrained minimization routine[6] (CONMIN) through a geometry module. The flap hinge line deflection angles and angle of attack were used as decision variables in the optimization routine to define the camber and twist distributions to minimize drag for the wing. The actual optimization procedure consists of perturbing each of the decision variables independently to determine gradients. The direction and relative deflection magnitudes to change the decision variables are then computed from the gradients. The controlling module of CONMIN then changes the decision variables simultaneously until either the drag increases or a constraint is encountered. A new set of gradients, along with a new move direction, is then computed. If a constraint has been reached, a new direction is selected in an attempt to further reduce drag without violating the constraint. Physical limits of the flap deflections plus a maximum pitching moment limit were the constraints imposed on the design configurations. The pitching moment constraint was imposed on the design space to restrict the trim drag penalty incurred with anticipated aft wing loading. When the configuration drag cannot be reduced further without violating a constraint, the optimum camber distribution has been found. It should be noted that a local minimum may have been determined instead of a global minimum. Therefore, several optimizations with different starting conditions may be required by some problems to determine the optimum configuration.

Six primary design points were targeted for wing optimization. These consisted of 0.2, 0.4, and 0.6 lift coefficients at a subsonic ($M=0.6$) and a transonic ($M=0.9$) Mach number. The Woodward-Carmichael linear theory code was used for the subsonic optimizations and to provide a set of starting cambers for the transonic optimization. The original plan for the transonic optimizations was to fix the leading-edge camber at the starting value and allow only the trailing edge to be optimized. Next, the trailing-edge optimized camber was fixed and the leading edge was optimized. In practice, the leading-edge flap deflections proved to be ineffective at reducing drag. This is probably a combination of two problems. Constraints on central processor time due to the number of flowfield solutions necessary for each optimization iteration required the solution mesh to be coarser than would be desirable for accurate configuration analysis. This, in conjunction with the small perturbation assumption of the Bailey-Ballhaus code, caused inaccuracies near the leading edge. Hence, the design approach may not have allowed the leading edge to be effective since the first step (trailing-edge optimization) drove the solution to a local minimum where improvements were the same order of magnitude as the accuracy of the force prediction capability of the analysis code. These factors prompted a decision to hold the leading edge to the camber defined by linear theory and optimize only the four trailing-edge flap segments.

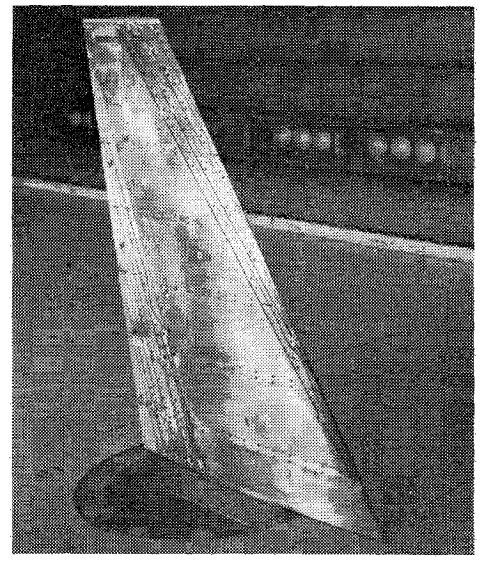

Fig. 2 Wind-tunnel installation.

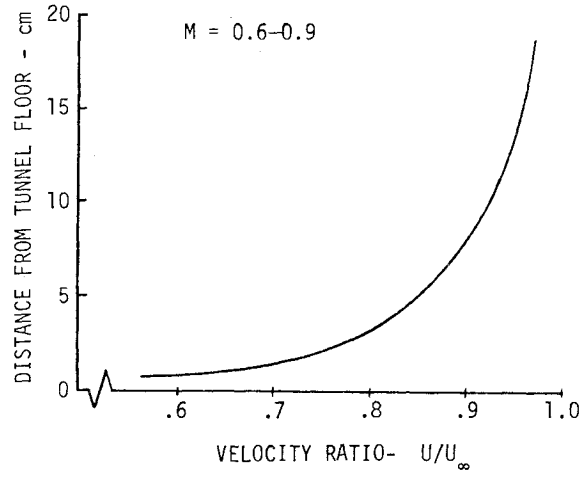

Fig. 3 Velocity distribution in the vicinity of the wind-tunnel floor.

Experiment

A test[7] was conducted in the NASA Ames 14-ft transonic tunnel to verify both the subsonic and transonic optimizations. Testing the semispan model in this tunnel posed some unique installation problems primarily related to the boundary layer on the tunnel floor. Several solutions were considered, with the final decision being to mount the 106.68-cm (42-in.) semispan model directly to the tunnel floor (see Fig. 2). The porous tunnel floor was covered with steel plates which acted as the configuration plane of symmetry. Provisions were included in the test schedule to investigate the boundary layer on the tunnel floor at the location of the model. These data are presented for the range of design Mach numbers in Fig. 3. Although the boundary-layer rake used did not encompass the entire boundary layer, enough data were obtained to estimate a displacement thickness of approximately 3.18 cm (1.25 in.).

The test schedule included seven optimized configurations, the best two configurations which had previously been tested during the NASA Langley test of the wing and a series of configurations used to experimentally verify an optimization. These were tested over the Mach range from 0.6 to 0.9, with data on most configurations obtained at 0.6, 0.7, 0.85, and 0.9 Mach numbers. Force and pressure data were obtained along with wing root bending moment and accelerometer data. The pressures were measured at 269 points distributed

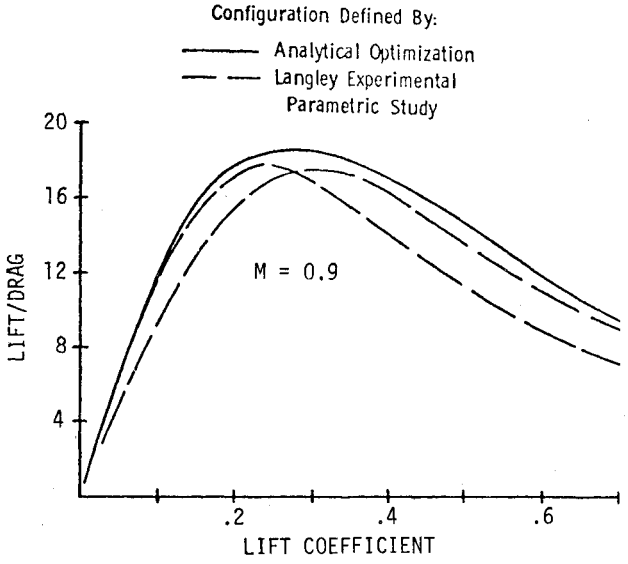

Fig. 4 Experimental lift-to-drag ratio comparison of Ames optimization test configuration.

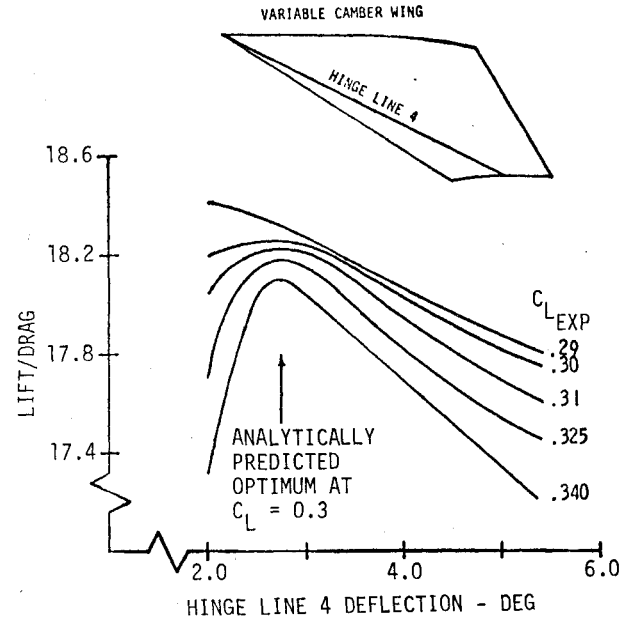

Fig. 5 Comparison of experimental and computational one hinge line optimization.

over the wing's upper and lower surfaces along seven spanwise stations.

At each design point, the analytically defined configurations proved to be as efficient, as indicated by the lift-to-drag ratio, as the best configurations from the Langley test. In addition, the optimized configurations had far better off-design characteristics, although off-design points were not used in defining the design space. This observation of off-design performance should not be used out of context, nor should it be inferred that this is typical of these types of comparisons. However, it is highly desirable in many cases to use off-design points as actual constraints in defining the design space. Presented in Fig. 4 are the lift-to-drag ratios for the two best configurations from the Langley experimental parametric study compared with data for one of the best configurations from the present study. These results would have been more dramatic had either the pitching moment constraint in the optimization been removed or an effective leading-edge optimization been performed. Possibly a different problem formulation could also have been used. For example, instead of limiting the pitching moment to a specific value, the pitching moment could have been trimmed by assuming some tail effectiveness and moment arm. This would have had the effect of altering the design space instead of bounding the feasible region with constraint lines.

In order to validate the analytically predicted configuration optimum, a simple study was conducted during the testing to determine an experimental optimum. An analytical optimum had been predicted at 0.3 C_L using only one of the wing hinge lines and angle of attack as decision variables. This configuration was tested along with three variations of the configuration. These were derived by varying the subject hinge line over a range of deflection angles which encompassed the expected optimum at the design lift coefficient. The variation of lift-to-drag ratio as a function of hinge line deflection at constant lift levels is presented in Fig. 5. Superimposed on the experimental data is an indication of the analytically predicted optimum hinge line deflection at 0.3 C_L. The results of the experimental and analytical optimization agree quite well at the design C_L.

Wing Optimization Comparisons

The initial optimization procedure did not allow for potential flow solutions to be obtained on a fine grid or to be carried to a high degree of convergence. Each run, which consisted of three optimization iterations using a relatively crude grid and liberal convergence criterion, required approximately 1 hour of CDC-7600 central processor time. Economics forced the optimizations to be performed in this manner, although it was recognized that relaxation solutions to classical three-dimensional small-disturbance (CSD) theory are compromised under these conditions. In this instance, the crude mesh degraded the solution accuracy near the wing leading edge, and the lack of convergence affected the repeatability and introduced noise into the design space. In order to verify the analytical predictions, it was desirable to analyze the configurations on a much finer grid network and allow the solutions to be relaxed to a smaller residual (indication of convergence). In addition, improvements had been incorporated into the analysis code, making the improved code attractive to use during the verification phase. A modified small-disturbance (MSD) equation, derived by retaining two previously neglected terms, enhanced the solution in regions along the span where the flow is essentially two dimensional in a plane normal to the sweep direction. A complementary finite differencing scheme was also incorporated into the coding.[8] This was necessary to insure suitable stability and shock capturing properties and to avoid excessive distortion of the shock profile.

The Bailey-Ballhaus analysis code is a very flexible analytical tool. Users are allowed interactions which can influence the accuracy and convergence rate through variations in grid spacing, convergence criteria, relaxation parameters, etc. Enough flexibility is allowed that it is possible to "fine-tune" a solution. An example of this could be concentrating grid points near an expected shock to improve the flowfield prediction in the vicinity of the shock wave. This is certainly advantageous in many cases; however, these analyses would be more meaningful if the solutions were influenced only by geometric differences in the various configurations. Therefore, a set of computational ground rules was established to insure that equal attention would be given to each of the analysis configurations. Essentially, these entailed holding constant all the program variables that were not geometry-dependent. In addition, comparisons with experimental data were to be made at the same lift coefficient. Viscous effects cause wing loadings to be lower than predicted by potential flow theory when compared at the same angle of attack. This anomaly, coupled with the fact that the wind-tunnel flow angularities and wall interference were not well defined, made it desirable not to tie the comparisons to a

Table 1 Configurations for comparison of variable camber pressure distributions with theoretical predictions

Configuration	Mach	C_L	Deflection angle[a] δ_1	δ_2	δ_3	δ_4	δ_5	δ_6	δ_7	δ_8
A92	0.9	0.2	0.2	0.6	1.3	2.0	1.6	1.2	0.5	0.8
A62	0.9	0.3	0.3	0.9	1.8	2.9	2.2	1.7	1.1	0.5
A94	0.9	0.4	0.3	0.8	1.7	2.7	2.0	1.4	1.4	6.2
A94	0.9	[b]	0.3	0.8	1.7	2.7	2.0	1.4	1.4	6.2
A94W	0.9	0.4	0.3	1.0	1.8	2.8	2.7	2.2	1.5	0.8
L5/T0	0.9	0.2	8.9	3.8	2.1	0.8	0.	0.	0.	0.
L5/T0	0.9	0.3	8.9	3.8	2.1	0.8	0.	0.	0.	0.

[a] For δ_1-δ_4, leading-edge down deflections are positive. For δ_5-δ_8, tailing-edge down deflections are positive.
[b] Comparisons between experiment and theory are at $\alpha = 3.5$ deg.

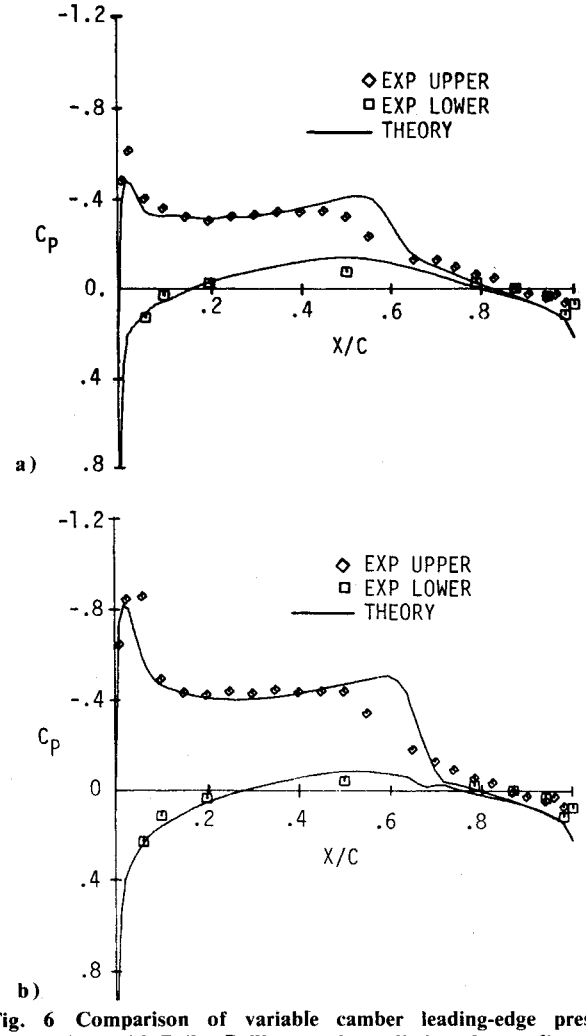

Fig. 6 Comparison of variable camber leading-edge pressure distributions with Bailey-Ballhaus code predictions for configuration L5/T0: a) $C_L = 0.2$, $M = 0.9$, ETA = 0.4; b) $C_L = 0.3$, $M = 0.9$, ETA = 0.4.

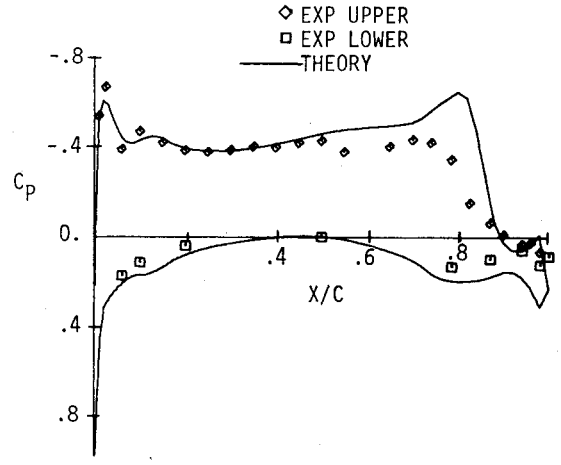

Fig. 7 Comparison of variable camber leading-edge pressure distribution with Bailey-Ballhaus code prediction for configuration A94: $M = 0.9$, ETA = 0.4, $\alpha = 3.15$ deg.

specific angle of attack, but rather to use wing lift coefficient as the common denominator.

The design configurations included in the analyses are presented in Table 1 along with a listing of the flap hinge line deflections defining the camber distributions for each of the configurations. The salient features of the comparisons of theory and experiment[9] are summarized below and illustrated by examples.

In previous analysis attempts, using the original Bailey-Ballhaus code at Vought, the prediction of flow expansion over the wing leading edge had not been entirely satisfactory. The present analysis showed remarkably good agreement near the leading edge (see Figs. 6a and 6b). This is particularly impressive considering the small-disturbance assumption inherent in the governing equation. It is interesting to note the comparison in Fig. 7 which presents a comparison at the same geometric angle of attack rather than the same lift coefficient. The excellent agreement at the section leading edge, due to the angle of attack being the same, is offset by a higher loading predicted over the remainder of the chord. Three major factors contribute to the leading-edge agreement observed in all of the comparisons: code improvements, mesh density in the forward 10% of the chord, and the relatively thin nature of the leading edge for the subject wing.

The theory tended to predict shocks located aft of the experimental shock position. This trend was most prevalent at inboard span stations (see Fig. 8a) and dissipated progressing outboard along the span (see Fig. 8b). These differences can be attributed to several factors. 1) The shock/boundary-layer interaction along the wind-tunnel floor (see Fig. 3) was not modeled in the computations, where the floor was the reflection plane for the isolated wing configuration. 2) Small differences in Mach number at the wing can cause large shifts in the shock location. For a two-dimensional airfoil, these shifts can be as large as 10% chord per 0.01 difference in Mach number.[10] During the experiment, it was not possible to monitor the local Mach number at the wing location. 3) Viscous effects on the wing surface tend to move the experimental shock wave forward. 4) More important than the preceding factors is the manner in which the comparisons were made. Matching wing lift coefficient causes the theory to compensate for underprediction in one region by overprediction in another region. Hence, if the loading at the leading edge is low, the theory will be pushed to a higher angle of attack. This shifts the theoretical shock aft and results in higher overall wing loading.

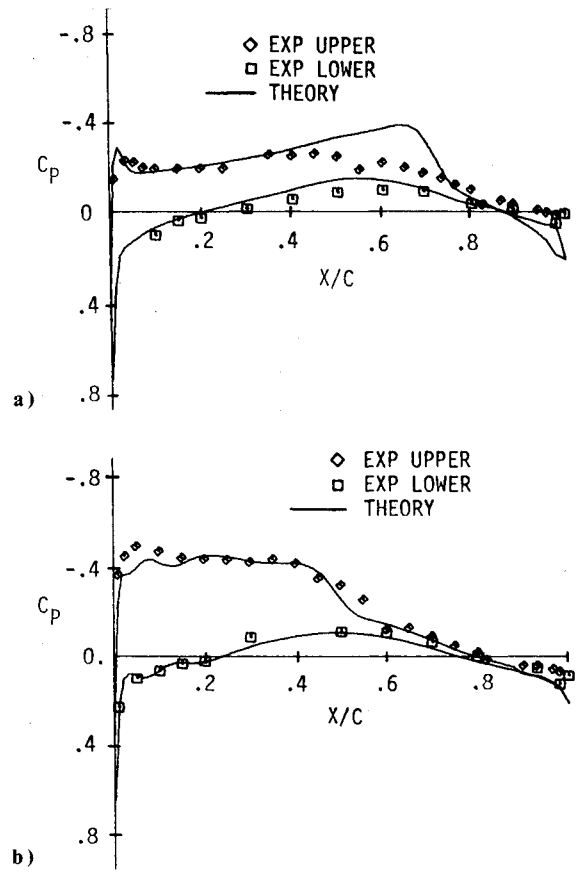

Fig. 8 Prediction of pressure distribution in the vicinity of a shock wave by the Bailey-Ballhaus code for configuration L5/T0: a) poor correlation at an inboard span station, $M=0.9$, ETA = 0.1, $C_L=0.2$; b) excellent correlation at an outboard span station, $M=0.9$, ETA = 0.7, $C_L=0.2$.

Conclusions

Study results indicate that numerical optimization can be both an effective and efficient design tool. The effectiveness is a direct function of the analysis used for the design. Essentially, this means the better the physics of the problem are modeled, the more effective the optimization will be. In general, this involves a tradeoff of cost (computer time) and solution accuracy. However, as efficient refinements are included in the analysis codes, an improved resolution at reduced cost is possible. An example is the imbedded mesh technique,[11] which has been incorporated into the latest Bailey-Ballhaus code since the comparisons presented here were completed. The comparisons of experimental and theoretical pressure distributions were very good when the improved code was used. This included prediction of shock location and the pressure jumps across the shocks, as well as the flow expansion about the wing leading edge. The best overall comparisons were made when the experiment and theory were compared at the same lift coefficient. The optimized configurations had as good or better lift-to-drag ratios at the design points as configurations which had been tested during an extensive experimental parametric study. The characteristics of the optimized configurations at points away from the design points were generally much better than the parametrically defined configurations.

Acknowledgments

The authors acknowledge the consulting assistance of R. Hicks (NASA Ames) and the substantial computer programming efforts of J. Frick (Informatics, Inc., Palo Alto, Calif.).

References

[1] Hicks, R.M. and Vanderplaats, G.N., "Application of Numerical Optimization to the Design of Supercritical Airfoils Without Drag Creep," SAE Paper 770440, Business Aircraft Meeting of the SAE, Wichita, Kans., March 29-April 1, 1977.

[2] Ferris, J.C., "Wind-Tunnell Investigation of a Variable Camber and Twist Wing," NASA TN D-8475, Aug. 1977.

[3] Ballhaus, W.F. and Bailey, F.R., "Numerical Calculation of Transonic Flow About Swept Wings," AIAA Paper 72-677, Boston, Mass., June 1972.

[4] Ballhaus, W.F. and Bailey, F.R., "Relaxation Methods for Transonic Flow About Wing-Cylinder Combinations and Lifting Swept Wings," *Lecture Notes in Physics,* Vol. 19, Springer-Verlag, 1972, pp. 2-9.

[5] Woodward, F.A., "A Unified Approach to the Analysis and Design of Wing-Body Combinations at Subsonic and Supersonic Speeds," *Journal of Aircraft,* Vol. 5, Nov.-Dec. 1968, pp. 528-534.

[6] Vanderplaats, G.N., "CONMIN-A FORTRAN Program for Constrained Function Minimization, Users Manual," NASA TM X-62, 282, Aug. 1973.

[7] Waggoner, E.G., Haney, H.P., and Ballhaus, W.F., "Wind-Tunnel Investigation of Computationally Optimized Variable Camber Wing Configurations," NASA TM 78,479, 1978.

[8] Ballhaus, W.F., Bailey, F.R., and Frick, J., "Improved Computational Treatment of Transonic Flow About Swept Wings," *Advances in Engineering Sciences,* Vol. IV, NASA CP-2001, 1976, pp. 1213-1231.

[9] Waggoner, E.G., Haney, H.P., and Ballhaus, W.F., "Computational Wing Optimization and Comparisons with Experiment for a Semi-Sapn Wing Model," NASA TM 78,480, 1978.

[10] Blackwell, J.A. and Pounds, G.A., "Wind-Tunnel Wall Interference on a Supercritical Airfoil at Transonic Speeds," *Proceedings of AIAA 9th Aerodynamic Testing Conference,* Arlington, Texas, June 1976, pp. 1-11.

[11] Boppe, C.W., "Calculation of Transonic Wing Flows by Grid Imbedding," AIAA Paper 77-207, Los Angeles, Calif., Jan. 1977.